MecSol2013
International Symposium on Solid Mechanics
April 18-19, 2013
Porto Alegre, Rio Grande do Sul, Brazil

# Comparison of Analytical and Numerical Solutions of Acoustic and Vibro-acoustic Cavities

**Álvaro Campos Ferreira, Marcus Vinicius Girão de Morais**
Department of Mechanical Engineering
Universidade de Brasília
alvaro.campos.ferreira@gmail.com

**Paulo Marcelo Vieira Ribeiro**
Departamento de Engenharia Civil
Universidade Federal de Pernambuco
paulo.vribeiro@ufpe.br

**Lineu José Pedroso**
Departamento de Engenharia Civil
Universidade de Brasília
lineu@unb.br

## ABSTRACT

The current work presents the comparison between analytical and numerical solutions of a vibro-acoustic cavity. The geometry used has been studied for many institutions (ITA, UFSC, USP) [4] in the research its acoustic properties. Its relative simplicity make it suitable not only for a numerical approach but for an analytical solution of its vibro-acoustic properties. The numerical models of interest include a completely rigid model, in which none of the walls will resonate with the cavity, and a vibro-acoustic model in which all but one wall will be rigid, the remaining wall will be flexible. The numerical model was done using FE-FSI which is implemented in the commercial software ANSYS 13.

**Keywords:** fluid-structure interaction, pseudo-coupled method, modal analysis, finite element

## 1 INTRODUCTION

The interest of acoustical modal analysis lies in the identification of low- (LF band) and mid-frequencies band (MF band) [1],[2].When pure or narrow band tones and its harmonics (LF band) associated to the firing frequency of engine excite the passenger cavity, this results in an increase of sound intensity. Several recent research projects, e.g. MID-Frequency [1] concentrate its attentions in the LF and MF band frequencies.

An analytical model was created using the separation of variables technique for the wave equation and using an imposed deformation function at the fluid-structure interface [3]. This solution enables the possibility of numerous boundary conditions for the bidimensional cavity modeled, including the case of closed and open cavities.

The current work presents the comparison between analytical and numerical solutions of a vibro-acoustic cavity. The geometry used has been studied for many institutions (ITA, UFSC, USP) [4] in the research its acoustic properties. Its relative simplicity make it suitable not only for a numerical approach but for an analytical solution of its vibro-acoustic properties. The numerical models of interest include a completely rigid model, in which none of the walls will resonate with the cavity, and a vibro-acoustic model in which all but one wall will be rigid; the remaining wall will be flexible. The numerical model was done using FE-FSI which is implemented in the commercial software ANSYS 13.

## 2 ANALYTICAL SOLUTION

The problems of dynamic fluid-structure interactions are of great interest to a wide range of research fields in engineering. In these cases, the movement of these two subsystems is not independent and is governed by dynamic contact conditions. According to Amabili and Kwak (*apud* Ribeiro, 2010) [3], analytical procedures show its importance in the solution of simple cases and can be used in the validation of numerical solutions.

The basic assumptions of this problem are the corresponding to treatment of this medium as an acoustic fluid. With these considerations, it is assumed that the fluid transmits only pressure waves. Some applications of this theory include propagation of pressure waves in pipes and sound waves propagating through fluid-solid media. The previous assumptions lead to a dynamic pressure distribution $p(x, y, t)$, in excess of the static pressure [5].

$$\nabla^2 \mathrm{p} = \frac{1}{\mathrm{c}^2}\frac{\mathrm{d}^2\mathrm{p}}{\mathrm{dt}^2} \tag{1}$$

Equation (1) corresponds to the wave equation where $\nabla^2$ is the bidimensional Laplacian operator and $c = \sqrt{\zeta/\rho_f}$ represents the fluid sound velocity, where $\zeta$ indicates the fluid bulk modulus and $\rho_f$ its density.

Equation (1) is achieved using the separation of variables technique, which assumes the equation can be separated, thus

$$\mathrm{p(x, y, t) = F(x)G(y)T(t)} \tag{2}$$

Substitution of(2) in(1) provides

$$\mathrm{F''(x)G(y)T(t) + F(x)G''(x)T(t)} = \frac{1}{\mathrm{c}^2}\mathrm{F(x)G(y)T''(t)} \tag{3}$$

The tiles indicate derivatives to the corresponding variable. Dividing equation(3) by $\mathrm{F}(x)G(y)T(t)$ gives

$$-\frac{\mathrm{G''(y)}}{\mathrm{G(y)}} = \frac{\mathrm{F''(x)}}{\mathrm{F(x)}} - \frac{1}{\mathrm{c}^2}\frac{\mathrm{T''(t)}}{\mathrm{T(t)}} \tag{4}$$

Analysis of equation(4) shows that this equation must be equal to an arbitrary constant $\beta$, which can assume positive negative or null values, once the left-hand side of this equation depends only on $y$ and the right hand depends on $x$ and $t$.

$$-\frac{\mathrm{G''(y)}}{\mathrm{G(y)}} = \beta \tag{5}$$

$$\frac{\mathrm{F''(x)}}{\mathrm{F(x)}} = \beta + \frac{1}{\mathrm{c}^2}\frac{\mathrm{T''(t)}}{\mathrm{T(t)}} = \alpha \tag{6}$$

$$\frac{\mathrm{T''(t)}}{\mathrm{T(t)}} = \mathrm{c}^2\left[\frac{\mathrm{F''(x)}}{\mathrm{F(x)}} - \beta\right] = \delta \tag{7}$$

Where $\alpha$, $\beta$ and $\delta$ are arbitrary separation constants. A simple and time independent solution for this problem can be achieved with the hypothesis of time harmonic vibrations, with frequency $\omega$. Thus it is assumed that the time-related function is given by

$$\mathrm{T(t)} = \mathrm{e}^{-\mathrm{i}\omega \mathrm{t}} \tag{8}$$

The relationship between the separation constants in the time harmonic problem should be clear:

$$\alpha = \beta - \frac{\omega^2}{c^2} \tag{9}$$

If we choose to solve this equation with

$$\beta = \left(\frac{n\pi}{L_y}\right)^2 = \kappa^2 \tag{10}$$

Then $F(x)$ and $G(y)$ become

$$G(y) = A\, cos(\kappa y) + B\, sin(\kappa y) \tag{11}$$

$$F(x) = C\, cos(\sqrt{\alpha}x) + D\, sin\left((\sqrt{\alpha}x)\right) \tag{12}$$

Where$A$,$B, C$ and $D$ are constants given by the boundary conditions of the problem. In each example, the structural vibrating boundary surface will be assumed to be governed by a time harmonic function, which provides us with a vibrating boundary acceleration related to an arbitrary shape function $\emptyset(y)$ [3]:

$$\ddot{u}(y,t) = \emptyset(y)\bar{A}e^{-i\omega t} \tag{13}$$

## 2.1 Entirely Open Cavity

For this case, all but one side of the cavity are assumed to be entirely open. The remaining side is assumed to be vibrating boundary. This solution was already studied in [3].

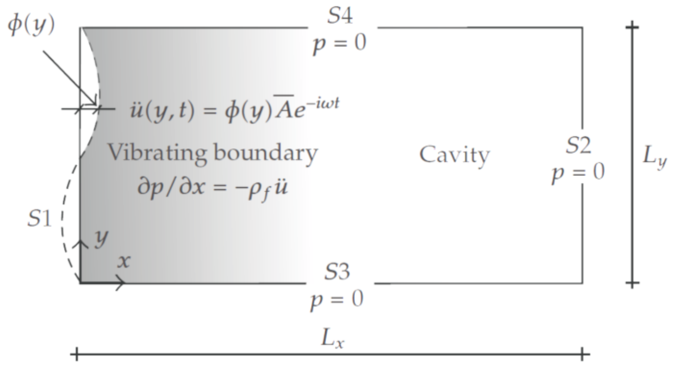


Figure 1 – Boundary conditions for an entirely open cavity and a vibrating boundary

For the boundary conditions given in Figure 1, substitution in equations (11) and (12), solving for every non-trivial solution gives

$$P(x,y) = \sum_{n=1}^{\infty} E_n.\left[sin(\sqrt{\alpha_n}.x) - tan(\sqrt{\alpha_n}.L_x)\, cos(\sqrt{\alpha_n}.x)\right] sin(\kappa.y) \tag{14}$$

Where $E_n$ is obtained using the boundary condition in the surface S1:

$$E_n = -\frac{2\rho_f \bar{A}}{L_y\sqrt{\alpha_n}}\int_0^{L_y} \emptyset(y)\, sin(\kappa.y)\, dy \tag{15}$$

Substitution of equation (15) in (14) provides the solution for the acoustic pressure in the entirely open cavity.

### 2.2 Closed Cavity in the Transversal Direction

In this case the boundary conditions for the cavity are the following pair of boundary conditions in the *x* and *y* directions, respectively: vibrating boundary-open and closed-closed [3].

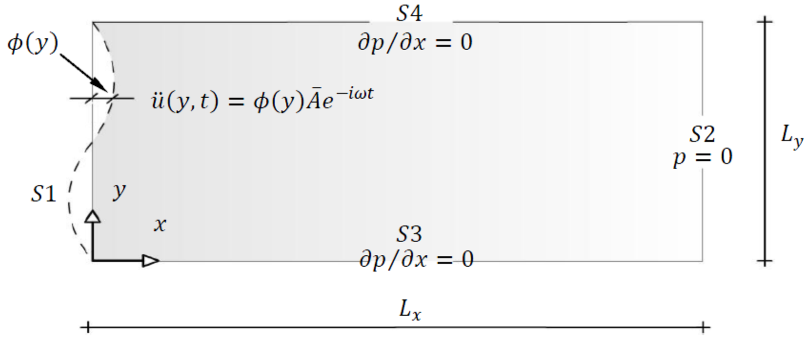


Figure 2 – Boundary conditions for a closed cavity in the transversal direction

Solving equations (11) and (12) for the boundary conditions shown in Figure 2 provides

$$P(x,y) = \sum_{n=0}^{\infty} E_n.\left[sin\left(\sqrt{\alpha_n}.x\right) - tan\left(\sqrt{\alpha_n}.L_x\right).cos\left(\sqrt{\alpha_n}.x\right)\right] cos(\kappa.y) \tag{16}$$

The component $E_n$ is obtained with the application of the boundary condition in S1:

$$E_0 = -\frac{\rho_f \bar{A}}{L_y\sqrt{\alpha_0}}\int_0^{L_y} \emptyset(y)dy\,, \qquad n = 0 \tag{17}$$

$$E_n = -\frac{2\rho_f \bar{A}}{L_y\sqrt{\alpha_n}}\int_0^{L_y} \emptyset(y)\cos(\kappa.y)\,dy\,, \qquad n = 1,2,3\ldots \tag{18}$$

### 2.3 Entirely Closed Cavity

For a cavity which has rigid walls in all of its surfaces with the exception of the vibrating boundary S1, the boundary conditions are shown in [6].

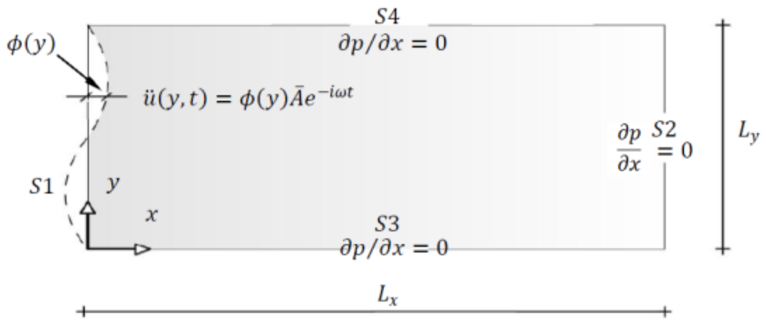


Figure 3 – Boundary conditions for an entirely closed cavity

$$P(x,y) = \sum_{n=0}^{\infty} E_n\left[sen\left(\sqrt{\alpha_n}\,x\right) + \frac{cos\left(\sqrt{\alpha_n}\,x\right)}{tan\left(\sqrt{\alpha_n}\,L_x\right)}\right] cos(k_n y) \tag{19}$$

The component $E_n$ is obtained with the application of the boundary condition in S1, which are the same as in the case 2.2, so the same equations (17) and (18) may evaluate $E_n$.

## 2.4 FLUID-STRUCTURE COUPLED SOLUTION FOR AN IMPOSED DEFORMATION

According to [3] the analysed problem can be illustrated as shown in Figure 4. It consists of a general structure with a constant cross-section subjected to an external load. The dynamic response of this system can be represented by a generalized coordinate $\mathrm{X}(t)$, allowing the construction of generalized parameters (mass, stiffness, and loading) for any arbitrary mode shape, related to $\emptyset(y)$. This type of solution will be very useful for the introduction of fluid pressures, since the previous developed approach for the fluid domain is also dependent on the shape function.

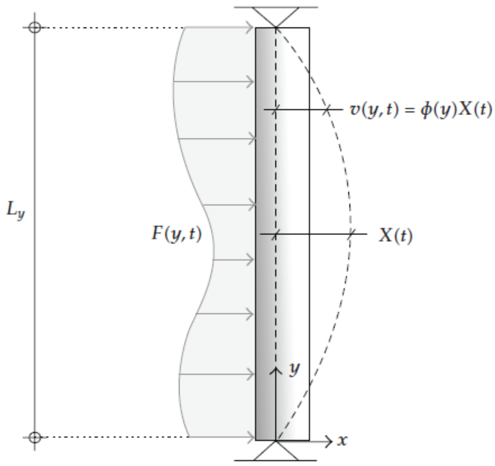


Figure 4 – Schematic representation of the structural model

Considering the new generalized coordinate $\mathrm{X}(t)$, it's possible now to describe the problem of the dynamic equilibrium as follows:

$$\widetilde{M}\ddot{X} + \widetilde{K}\mathrm{X} = \tilde{F}(y,t) \tag{20}$$

$$\widetilde{M} = \int_0^{L_y} \mu(y)[\emptyset(y)]^2 dy \tag{21}$$

$$\widetilde{K} = \int_0^{L_y} EI(y)\left[\frac{\mathrm{d}^2\emptyset(y)}{dy^2}\right]^2 dy \tag{22}$$

$$\tilde{F} = \int_0^{L_y} F(y,t)\emptyset(y)dy \tag{23}$$

Where $\widetilde{M}$, $\widetilde{K}$ and $\tilde{F}$ are related, respectively to generalized mass, generalized stiffness and generalized loading, $\mu$ is the linear density of the structure, $EI$ is the flexural rigidity of the structure. This solution depends on an external loading. In the case of a coupled system this loading is represented by the dynamic pressures acting at the interface. Therefore:

$$\mathrm{F}(y,t) = p(0,y,t) = P(0,y)e^{-i\omega t} \tag{24}$$

$$\ddot{X} = \bar{A}e^{-i\omega t} \tag{25}$$

Where $P(0,y)$ is the function related to the corresponding cavity and its boundary conditions. For the harmonic problem with a natural frequency of $\omega$ [7]:

$$\widetilde{M}_{total}\ddot{X} + \widetilde{K}\mathrm{X} = 0 \tag{26}$$

Where

$$\widetilde{M}_{total} = \widetilde{M} + \int_0^{L_y} \frac{P(0,y)}{\bar{A}}\emptyset(y)dy \tag{27}$$

This results in:

$$\widetilde{K} - \omega^2 \widetilde{M}_{total} = 0 \tag{28}$$

Solution of equation (28) provides the frequencies of the coupled problem.

### 2.5 Application of a Deformation Function

Up until now, the deformation function used in the boundary surface S1 was arbitrary with the only assumption being that it was governed by a time harmonic function and an arbitrary shape function. For the cases studied in this article, a sinusoidal shape function will be assumed for this deformation function. Thus,

$$\emptyset(y) = \sin\left(\frac{j\pi y}{L_y}\right) \tag{29}$$

This shape function is appropriate for the approximation of the deformation of a two-dimensional beam.

## 3 RESULTS

From each boundary condition, an analytical and a numerical solution were developed and their results were compared in a way that both the mode shape and the mode frequency were taken in account. The fluid-structure coupled solution for an imposed deformation was able to reproduce with relative precision as seen below in Table 2, Table 4 and Table 6. For each boundary condition, a different set of material properties was used for the fluid and for the structure. These different properties were chosen to validate the method using different models and obtaining different results. Figure 5 shows the geometric properties which will be referenced throughout the cases. For the meshing in the numerical cases, 20 elements were used in each surface, with a total of 400 fluid elements and 20 structure elements. The fluid element used was FLUID29 and the structure element was BEAM3. The colour scheme in the analytical solution is slightly different than the scheme in the numerical solution; each result will be discussed in its topic.

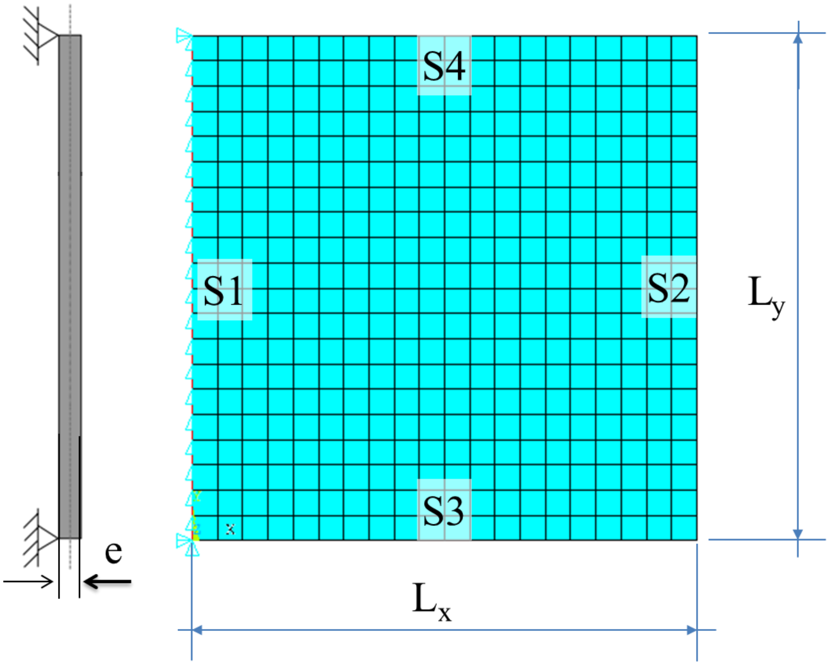


Figure 5 – Mesh created for the numerical analysis and beam properties.

### 3.1 CASE 1 – Entirely Open Cavity

This case corresponds to the boundary conditions exposed in section 2.1. All of the geometric and material properties are listed in Table 1. In each case it's noticeable that the acoustic pressure at the surfaces S2, S3 and S4 are all zero.

Table 1 – Geometric and Material properties for Case 1

| Geometric Data | Fluid Domain | Solid Domain |
|---|---|---|
| $L_x = L_y = 10\ m$ | $\rho_f = 1000\ kg/m^3$ | $\rho_s = 7800\ kg/m^3$ |
| $e = 1.0\ m$ | $c = 1500\ m/s$ | $E = 2.1\ 10^{11}\ kg/m$ |
| $I_{yy} = \dfrac{e^3}{12}\ m^4$ | | |

Table 2 – Analytical – Numerical Comparison of the Solution for the Completely Open Cavity (frequency in Hz)

| Numerical Frequency | Analytical Frequency | Shape Function | Numerical Mode Shape | Analytical Mode Shape |
|---|---|---|---|---|
| 127,77 | 124,00 |  | 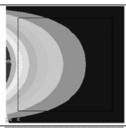 | 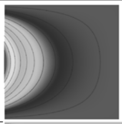 |
| 524,25 | 529,58 |  | 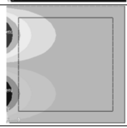 | 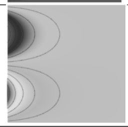 |
| 570,38 | 570,32 |  | 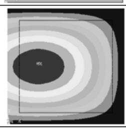 | 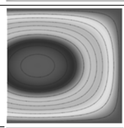 |
| 883,67 | 882,19 |  | 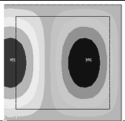 | 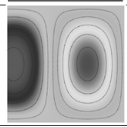 |
| 1005,00 | 1002,72 |  | 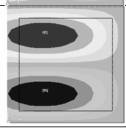 | 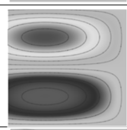 |
| 1167,29 | 1189,23 |  | 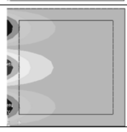 | 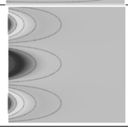 |

### 3.2 CASE 2 - Closed Cavity in the Transversal Direction

This case corresponds to the boundary conditions stated in section 2.2. It's noteworthy that for some cavity modes the fluid interaction will modify the beams shape mode as stated by [3]. In these cases, the imposed deformation method will be limited, once an unchanged in-vacuum mode shape of the beam is assumed. The imposed deformation method remains valid if a dominant configuration is established for the structure deformation. The method will still be able to produce an approximation of the acoustic mode shape for the cavity, but the overall results from these specific mode shapes will not correspond to reality. These effects are shown in modes 3 and 6 from Table 4. In mode 3, the imposed deformation method is still able to reproduce the result, once the structure mode shape still shows some dominance.

Table 3 – Geometric and Material properties for Case 3

| Geometric Data | Fluid Domain | Solid Domain |
|---|---|---|
| $L_x = L_y = 10\ m$ | $\rho_f = 1000\ kg/m^3$ | $\rho_s = 2000\ kg/m^3$ |
| $e = 1.0\ m$ | $c = 1500\ m/s$ | $E = 2.5\ 10^{10} kg/m$ |
| $I_{yy} = \dfrac{e^3}{12}\ m^4$ | | |

Table 4 – Analytical – Numerical Comparison of the Solution
for the Closed Cavity in the Transversal Direction(frequency in Hz)

| Numerical Frequency | Analytical Frequency | Shape Function | Numerical Mode Shape | Analytical Mode Shape |
|---|---|---|---|---|
| 43,71 | 43,68 |  | 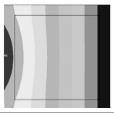 | 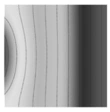 |
| 254,76 | 255,10 |  |  | 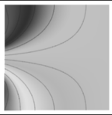 |
| 375,82 | 381,30 |  |  | 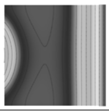 |
| 613,08 | 616,38 |  | 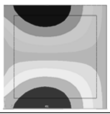 | 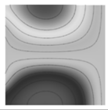 |
| 642,90 | 642,55 |  | 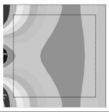 | 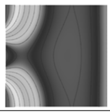 |
| 831,77 | 741,59 |  | 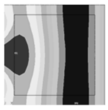 | 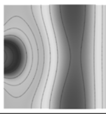 |
| 911,38 | 925,42 |  |  | 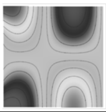 |

## 3.3 CASE 3 – Entirely Closed Cavity

This case corresponds to the boundary conditions stated in section 2.3. As it was noted in case 3.2, the imposed deformation method is not valid if the structures deformation does not have a dominant configuration. In these cases, the fluid interaction with the structure will produce a mixed mode shape for the structure, which is not considered in the imposed deformation method. This effect can be observed in modes 1 and 3, in which the imposed deformation method will not be able to provide the expected frequency, once the mode shape from the structure is not the unchanged in-vacuum, which is used in the imposed deformation method. This case was based in [8].

Table 5 – Geometric and Material properties for Case 3

| Geometric Data | Fluid Domain | Solid Domain |
|---|---|---|
| $L_x = L_y = 10\ m$ | $\rho_f = 1000\ kg/m^3$ | $\rho_s = 7800\ kg/m^3$ |
| $e = 1.0\ m$ | $c = 1500\ m/s$ | $E = 2.1\ 10^{11}\ kg/m$ |
| $I_{yy} = \dfrac{e^3}{12}\ m^4$ | | |

Table 6 – Analytical – Numerical Comparison of the Solution for the Completely Closed Cavity (frequency in Hz)

| Numerical Frequency | Analytical Frequency | Shape Function | Numerical Mode Shape | Analytical Mode Shape |
|---|---|---|---|---|
| 177,75 | 164,03 |  | 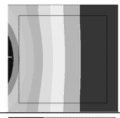 | 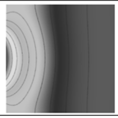 |
| 430,07 | 430,67 |  | 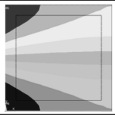 | 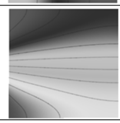 |
| 515,76 | 416,53 |  | 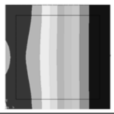 | 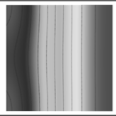 |
| 543,06 | 545,59 |  | 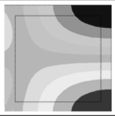 | 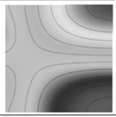 |
| 726,40 | 729,70 |  | 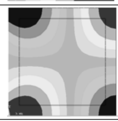 | 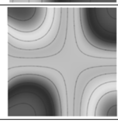 |
| 930,35 | 927,59 |  | 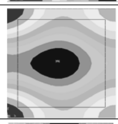 | 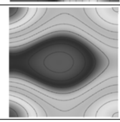 |
| 969,56 | 967,16 |  | 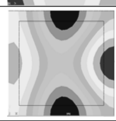 | 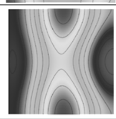 |

## 4 CONCLUSION

The present work validates a methodology to analyse the fluid-structure coupling effects in a closed cavity using the analytical pseudo-coupled method developed for an acoustic cavity and a structure submitted to an imposed deformation. This methodology can be useful in the analysis of several coupling problems of great relevance in the acoustics field.

The analytical pseudo-coupled method showed a good correlation with the coupled model discretized by a converged numerical model (ANSYS 13). The limitations of the simplified pseudo-coupled method were studied particularly in Case 2 and 3 in which structural shape modes weren't a simple sinusoidal function.

The next step is applied pseudo-coupled method to obtain a approximation of a tridimensional cavity, as described in [4]. A numerical, experimental and analytical comparison is intended.

## REFERENCES

[1] Dey, S.; Shirron, J. J. & Couchman, L. S., (2001), 'Mid-frequency structural acoustic and vibration analysis in arbitrary, curved three-dimensional domains', Computers and Structures, **79**(6), 617 – 629

[2] Soize, C., (1998), 'Reduced models in the medium frequency range for general dissipative structural-dynamics systems', European Journal of Mechanics - A/Solids, **17**(4), 657 – 685

[3] Ribeiro, P., (2010), Soluções Analíticas para Cavidades Acústicas Bidimensionais com Aplicação ao Estudo de Problemas de Interação Dinâmica Barragem-Reservatório, Departamento de Engenharia Civil e Ambiental, Universidade de Brasília, Brasília/DF

[4] Tourinho, A., (2011), 'Construção de Modelo para Análise de Funções de Transferência de Sistemas Vibro-Acústicos', Projeto de Graduação, Departamento de Engenharia Mecânica, Universidade de Brasília, Brasília/DF

[5] Kinsler, L.E., Frey, A. R ., Coppens, A.B., Sanders, J.V., (1999), 'Fundamentals of Acoustics', Wiley, New York

[6] Ferreira, A.C., (2012), 'Comparação Analítica Numérica de Cavidades Acústicas e Vibro-Acústicas', Projeto de Graduação, Departamento de Engenharia Mecânica, Universidade de Brasília, Brasília/DF

[7] Ribeiro, P. M. V. and Pedroso, L. J. , (2010), 'Solution of the Dynamic Interaction Problem between a Framed Structure and an Acoustic Cavity Using Imposed Deformation Functions at the Interface', Mathematical Problems in Engineering, Volume 2010, 1-33

[8] Souza, S.M., 2007, Pedroso, L.J., (2009), 'Study of Flexible wall acoustic cavities using Beam Finite Element', Mechanics of Solids in Brazil, 223-237